Journal of Photochemistry and Photobiology A: Chemistry 217 (2011) 267–270

Contents lists available at ScienceDirect

Journal of Photochemistry and Photobiology A: Chemistry

journal homepage: www.elsevier.com/locate/jphotochem

Short note

A simple CdS nanoparticles cascading approach for boosting N3 dye/ZnO nanoplates DSSCs overall performance

Swapnil B. Ambade[a,b], Rajaram S. Mane[a,d,1], Anil V. Ghule[a], Go-Woon Lee[c], Ramphal Sharma[a], Oh-shim Joo[c], Rohan B. Ambade[d,1], Soo-Hyoung Lee[b,*], Sung-Hwan Han[a,*]

[a] Inorganic Nano-Materials Laboratory, Department of Chemistry, Hanyang University, Haengdang-dong 17, Sungdong-ku, Seoul 133-791, Republic of Korea
[b] Organic Optoelectronic Materials Laboratory, Division of Semiconductor and Chemical Engineering, Chonbuk National University, Jeonju, Republic of Korea
[c] Clean Energy Research Center, Korea Institute of Science and Technology, Seoul 130-650, Republic of Korea
[d] School of Physical Sciences, Swami Ramanand Teerth Marathwada University, Nanded 431606, M.S., India

ARTICLE INFO

Article history:
Received 8 July 2010
Received in revised form 21 August 2010
Accepted 25 September 2010
Available online 1 November 2010

Keywords:
Chemical synthesis
Electron spectroscopy
Electrical properties
Surface properties

ABSTRACT

Enhanced photosensitization in presence of CdS nanoparticles is achieved in electrochemically deposited ZnO nanoplates and N3 loaded dye-sensitized solar cells. Chemically embedded CdS nanoparticles act as a sandwiching layer between ZnO nanoplates and dye molecules by overcoming current limiting serious Zn^{2+}/dye insulating complex formation and CdS photo-corrosion issues. The X-ray diffraction and the scanning electron microscopy confirm the ZnO with vertically aligned nanoplates, perpendicular to the substrate surface. Amorphous CdS is monitored using electron dispersive X-ray analysis. The low and high resolution transmission electron microscope images confirm the presence of CdS nanoparticles over ZnO nanoplates which later is supported by an increase in optical absorbance and shift in band edge. About 400% increase in solar conversion efficiency with this cascade arrangement is achieved when compared with without CdS which could be fascinating while designing solid state solar cells in presence of suitable *p*-type layer.

1. Introduction

Nanocrystalline mesoporous metal oxide-based dye-sensitized solar cells (DSSCs) are possibly the only validated alternative to currently used expensive silicon-based solar cells. As such they are not important in their own right, but serve as a useful stimulant to the innovation in emerging new trends of the solar cell developments. In a standard conventional photovoltaic device, the semiconductor layers absorb light producing electron–hole pairs, which are subsequently separated to provide a photovoltage by junctions, either with other semiconductors or Schottky contacts with metals. On the other hand, in the DSSCs system, the recombination loss mechanism need to be minimized, since the processes of optical absorption and charge separation takes place on distinct phases [1]. Till date, TiO_2 has been considered as an efficient candidate for DSSCs application because of its high solar-to-electrical energy conversion efficiency (η%), chemical stability and abundancy. Presently, other wide band gap energy metal oxides such as ZnO (3.2 eV), SnO_2 (3.5 eV), Nb_2O_5 (3.1 eV), etc. of different nanostructructures are also found to be of great practical interests. Despite unique electronic properties, good electron mobility, nearly same band gap energy and matching conduction band position, ZnO-based DSSCs systems show inferior performance than TiO_2. There is a need to elaborate this problem kinetically. To address this issue in depth, different nanoforms including nanocrystals [2], nanowires [3,4], nanotubes [4,5] and platelets (NPl) [6–8] of ZnO were employed to understand nanoform-based charge transportation. It is assumed and later proved that the hopping operation, caused by spherical nanocrystallites, is limiting the performance of DSSCs [3] when electrode consists of spherical nanocrysyallites. Secondly, formation of Zn^{2+}/dye complex, a relatively non-conductive/insulating layer blocks the overall electron injection efficiency of the dye molecules. This eventually leads to the inferior DSSCs performance. This can be minimized by incorporating the semiconductor nanoparticles (NPs) of relatively higher conduction band positions than used porous metal oxides [9]. Photo-degradation which eventually blocks the durability of photoelectrochemical cells is one of the serious problems in metal chalcogenides. For example in case of CdS, due to $CdS + h\nu \rightarrow CdS\,(h^+ + e^-)$ and $2h^+ + CdS \rightarrow S + Cd^{2+}$, where h^+, e^-, and S denote a hole in the valence band, electron in the conduction band, and a sulfur atom deposited on the electrode surface respectively, photo-corrosion is dominant. Therefore, there is a need to apply some strategy by which both effects should be minimized. In continuation to our research presented in past to achieve

* Corresponding authors. Tel.: +822 2220 2558; fax: +822 2299 0762.
E-mail addresses: shlee66@jbnu.ac.kr (S.-H. Lee), shhan@hanyang.ac.kr (S.-H. Han).
[1] Present address.

1010-6030/$ – see front matter © 2010 Elsevier B.V. All rights reserved.
doi:10.1016/j.jphotochem.2010.09.023

these requirements [10–13], in this communication, we present dual photosensitization in electrochemically developed ZnO NPl using CdS NPs and N3 dye, i.e. cascade system. Surface passivation of ZnO NPl is achieved by sandwiching the CdS NPs layer between ZnO NPl and N3 dye. Cascade system with descending energy levels, i.e. lowest unoccupied molecular orbit of dye followed by conduction bands of CdS NPs and ZnO NPl would favor fast charge transport to electrons collecting electrode. On account of favorable energy band positions the charge injection from one semiconductor into another leads to efficient charge separation by reducing the electron–hole pair recombination's [14,15]. It infers that this CdS NPs cascading process is minimizing greatly the formation of insulating ZnO NPl layer in N3 dye presence and overcome efficiency limiting complex formation activity [16,17] which is one of the serious challenges in ZnO-based DSSCs. Secondly and interestingly, by embedding CdS NPs between the ZnO NPl and N3 dye the additive hybrid organic/inorganic photosensitization effect can be achieved.

2. Experimental details

A simple electrochemical route was preferred to obtain ZnO NPl onto the transparent indium–tin–oxide (ITO) substrates. Cathodic potential of 1.1 V was applied in-between the counter (platinum spiral wire) and the working electrodes in presence of Ag/AgCl reference electrode. An aqueous solution composed of 0.05 M zinc nitrate and 0.1 M potassium chloride was maintained at 343 K and deposition was carried out for 1800 s. For embedding CdS NPs, room temperature (300 K) chemical bath deposition method involving solution mixture of 0.01 M $CdCl_2$ (ammonium hydroxide complexed) and 0.01 M thiourea was used [18]. The deposition was carried out for 50 min at room temperature (27 °C). The ZnO NPl–CdS NPs (ZnO–CdS) electrode was annealed at 473 K for 30 min. To address the issue of surface aggregation caused due to prolonged interaction between the ZnO NPl and N3 dye, ZnO NPl, ZnO–CdS electrodes were sensitized with ruthenium (II) *cis*-di(thiocyanato)bis(2,2′-bypyridyl-4,4′-dicarboxylic acid) (N3) dye for 20 h. X-ray diffraction (XRD) measurements were carried out using Philips, Japan MPD 1880, X-ray powder diffractometer [Cu Kα radiation, $V = 40$ kV and $I = 100$ mA] to confirm the formation of ZnO NPl electrodes. Using scanning electron microscope, SEM, JEOL, Japan, surface texture was identified. Electrode thickness was confirmed from the cross-sectional SEM image. Owing to the amorphous nature of the embedded CdS, energy dispersive X-ray analysis measurement was conducted to confirm its presence in the form of Cd and S. The optical absorption spectra for ZnO NPl, ZnO NPl–CdS NPs, ZnO NPl/N3 and ZnO NPl–CdS NPs/N3 electrodes were measured with UV-Vis spectrophotometer Hitachi-330 (Japan). The presence of CdS NPs over ZnO NPls was confirmed using electron transmission microscope (TEM) images at two different magnifications. Samples for TEM investigations were prepared by putting an aliquot of dichloromethane solution of ZnO NPl–CdS NPs onto an amorphous carbon substrate supported on a copper grid. The excess liquid was then wicked away with tissue, and the grid was allowed to dry at room temperature. Fast charge injection kinetics observed after including the CdS NPs sandwich layer between the ZnO NPl and N3 dye molecules layer was supported by cyclic-voltammetry (*CV*) measurements when compared with only ZnO NPl–N3 dye and ZnO–CdS, respectively. The measurements of the dye-sensitized solar cells were performed by illuminating the cells through the conducting glass surface using a 1-kW xenon lamp with a photointensity of 100 mW/cm^2 and an effective electrode area of 0.28 cm^2. 0.6 M 1-hexyl-2,3-dimethyl-imidazolium iodide (C6DMI), 0.1 M lithium iodide (LiI), 0.05 M iodide (I_2), and 0.5 M 4-tert-butylpyridine (*t*-BPy) in 15 mL methoxyacetonitrile (98%) was used as an electrolyte.

3. Results and discussion

Fig. 1a shows initial rapid surge and decay of the current density due to the double layer charging. Initially, the formation of $Zn(OH)_2$ nuclei by overcoming Helmholtz double layer could have affected on current density. Furthermore, due to steady nuclei growth current density increases exponentially with time. Thus, the cluster formation after double layer charging is an indication of critical nuclei formation. Diffusive controlled growth of the $Zn(OH)_2$ over the nuclei is responsible for $Zn(OH)_2$ NPl surface morphology. Annealing of $Zn(OH)_2$ NPl at 553 K for 1 h converted it into ZnO NPl (Fig. 1b), which is confirmed from the XRD pattern recorded at room temperature with a scan rate of 4°/min. The XRD pattern clearly shows the dominance of (1 1 0) and (1 0 1) peaks over (0 0 2) peak. The (0 0 2) peak is supposed to be a characteristic of ZnO nanorods-like nanostructure, thus, the presence of (0 0 2) peak with relatively lower intensity indicates the formation ZnO NPls electrode. The peak intensity of (0 0 2) plane in XRD pattern is in general sensitive to the concentration of oxygen vacancies. The higher the number of oxygen vacancies, lower is the resistivity and therefore, the best conducting electrodes should ideally have a zero peak intensity of (0 0 2) [19]. The peak positions, marked with filled circles, in the XRD pattern correspond to ITO, reference, reflections. The observed XRD pattern is in good agreement with that reported earlier (JCPDS 01-1136), confirming the formation of ZnO. Fig. 1c shows the representative SEM image of ZnO NPl electrode. The width of the vertically grown individual ZnO NPl is 100–150 nm. The inset clearly indicates that the thickness of the electrode is 5 (±0.5) μm. Due to amorphous nature of the CdS NPs, their formation over the ZnO NPl was confirmed using EDAX (Fig. 1d) spectrum. The quantitative elemental analysis of Zn, Cd, O and S was performed which shows the average atomic percentage for Zn:O:Cd:S is to be 47:49:2:2, supporting the formation of CdS NPs on ZnO NPl. Fig. 1e and f present the TEM images of ZnO NPl–CdS NPs scanned at two different magnifications. It is seen in the low magnified TEM image and later proved using optical absorbance that the CdS NPs are well-connected to the ZnO NPl. The CdS NPs look smaller in size than ZnO NPl. Uniformly spaced regular straight fringes correspond to *d* spacing of ZnO are clearly seen in the high resolution TEM image.

Fig. 2a shows the DSSCs performances of ZnO NPl/N3, ZnO–CdS, ZnO–CdS/N3 electrodes. The curve corresponding to ZnONPl/N3 dye indicates the short circuit current (J_{sc}) of 1.54 mA/cm^2, open circuit voltage (V_{oc}) of 0.47 V, fill factor (*ff*) of 0.42 and conversion efficiency (η) of 0.36%, respectively. This obtained lower observed conversion efficiency is attributed to the surface aggregation phenomenon noted as a result of Zn^{2+}/N3 complex insulating layer formation. On the other hand, in case of ZnO–CdS electrode electronic parameters are $J_{sc} = 0.50$ mA/cm^2, $V_{oc} = 0.27$ V, $ff = 0.31$ and $\eta = 0.04$%. Due to far UV light absorption the obtained smaller J_{sc} and V_{oc} values could have affected the conversion efficiency [20–22]. However, in the presence of CdS NPs as a sandwich layer between ZnO NPl and N3 dye molecules layer, substantial increase in current density due to the dual photosensitization and minimized surface aggregation is achieved. Hybrid CdS NPs and N3 dye absorption properties contribute in enhancing the overall current density. Looking once more at the *J–V* performance, on account of dual-photosensitization, the current density appears to be entirely dominated with of CdS NPs and N3 dye molecules immobilization that lead to get the J_{sc} of 7.84 mA/cm^2, V_{oc} of 0.54 V and η as high as 1.30%. In this case, the fill factor remains nearly the same, indicating that the CdS NPs layer provides effective coupling between ZnO NPl and N3 dye molecules and avoiding ZnO surface aggregation and thereby electrode series resistance. This reveals that ZnO–CdS/N3 electrode contributes towards the faster charge transfer kinetics as noted from the 5-fold increase in J_{sc} value, which in

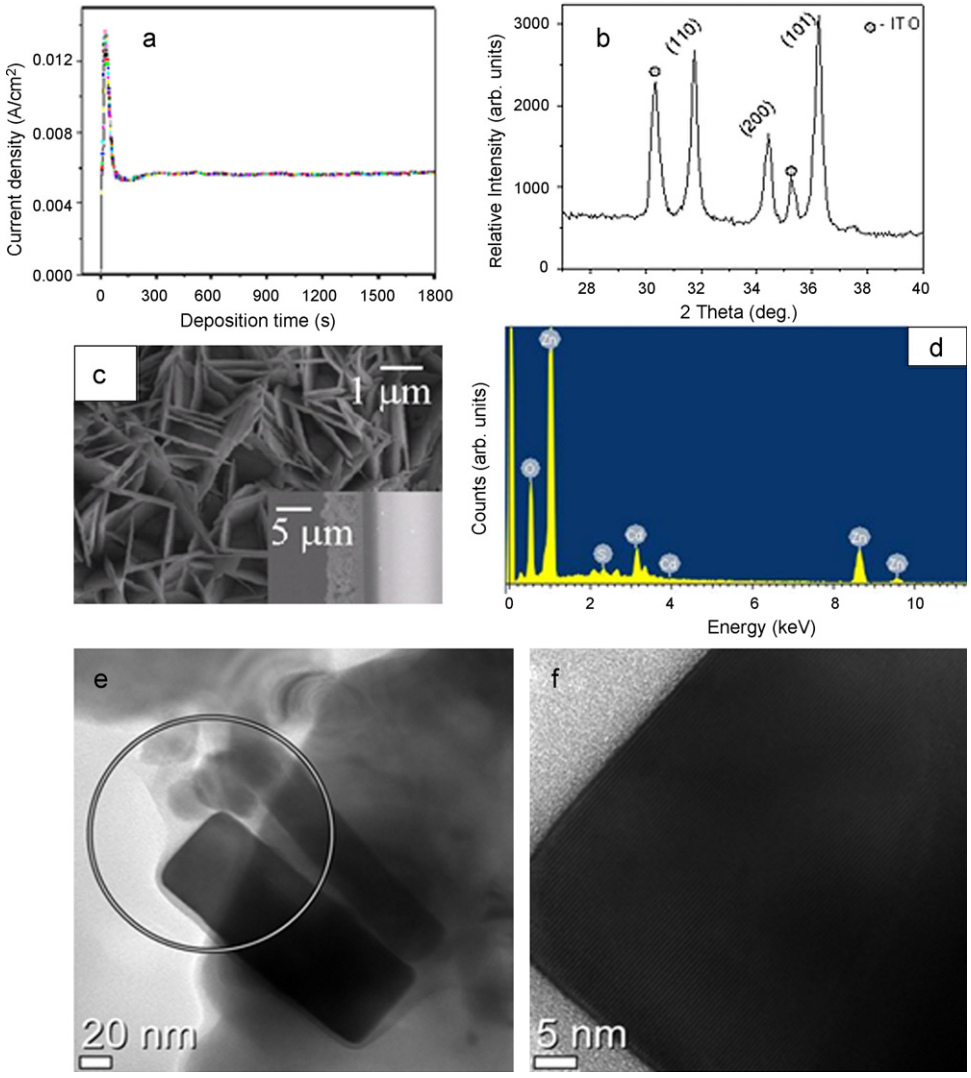

Fig. 1. (a) The current density variation as a function of time during the electro-deposition of ZnO nanoplates on the ITO substrate. (b) X-ray diffraction pattern confirming the formation of ZnO. (c) Representative SEM image showing the uniform surface morphology of the ZnO nanoplates electrode. Inset shows cross-section view of the ZnO NPl electrode indicating the average thickness of the electrode. (d) Energy dispersive X-ray analysis spectrum showing the presence of Zn, Cd, S and O elements, and also confirming the formation of CdS nanoparticles. (e) and (f) CdS NPs well-connected to ZnO NPl with regular straight fringes.

turn supports the additive-type sensitization of ZnO NPl. The electrons injected by N3 dye molecules into the CdS conduction band are transferred to the ZnO NPl through the intermediate cascade steps, unlike through the Zn^{2+}/dye complex insulating potential barrier layer in ZnO NPl/N3 [23,24]. Fig. 2b presents a stability test for 14 h. The ZnO NPl/N3 electrode shows good stability but smaller current density due to formation of Zn^{2+}/dye aggregation layer. Because of inherent defects present in the CdS, a considerable loss of the photo-generated charge carriers is noted as a result of charge recombination, leading to poor electrochemical stability of ZnO–CdS electrode. The anodic reaction at the surface of ZnO–CdS electrode on illumination is known to cause dissolution of CdS on the electrode surface [25]. Therefore, for the stability of ZnO–CdS electrode, surface dissolution of CdS in light should be suppressed. As expected, ZnO–CdS/N3 electrode was considerably stable which is due to the effective coupling of N3 dye with ZnO NPl through carboxylic groups in presence of CdS NPs. The CdS NPs between ZnO NPl and N3 have prohibited a direct contact of N3 dye molecules with ZnO NPl which would have prevented both the CdS dissolution through photo-corrosion and also the ZnO NPl surface aggregation phenomena. The *CV* measurements (Fig. 2c) were performed using acetonitrile as a solvent with 0.1 M tetrabutylammonium/tetra-fluoroborate in the potential region from 0 to −1.8 V and scanning rate of 50 mV/s confirming the presence of CdS on ZnO NPl. As expected, due to more light harvesting potential (see the followed part), higher current density in ZnO–CdS/N3 electrode is observed wherein, the charge injection kinetics is faster (as evidenced from the *J–V* and stability measurements) compared to that of ZnO NPl/N3 and ZnO–CdS electrodes, respectively. The low current densities in ZnO NPl–CdS and ZnO NPl/N3 are attributed to (a) poor light absorption on account of single absorber and (b) complex insulating layer formation due to acidic nature of dye with ZnO, which is increased considerably after forming CdS and N3 bilayers due to establishment of favorable band positions that can facilitate easy transportation of injected charge carriers by reducing recombinations with dye molecules and iodine species in electrolyte. Fig. 2d shows optical absorbance of four electrodes viz, pristine ZnO NPl, ZnO NPl–CdS NPs, ZnO NPl/N3 and ZnO NPl + CdS NPs + N3 wherein, the sharp absorbance at about 380 nm corresponding to 3.26 eV is confirmed. The band edge of about 100 nm is shifted to a higher wavelength due to linking of CdS NPs. However, within 380–480 nm wavelength the absorbance of ZnO NPl/N3 electrode is inferior, confirming the absence of CdS NPs over ZnO NPl whereas, ZnO NPl–CdS NPs electrode, N3 dye peak is

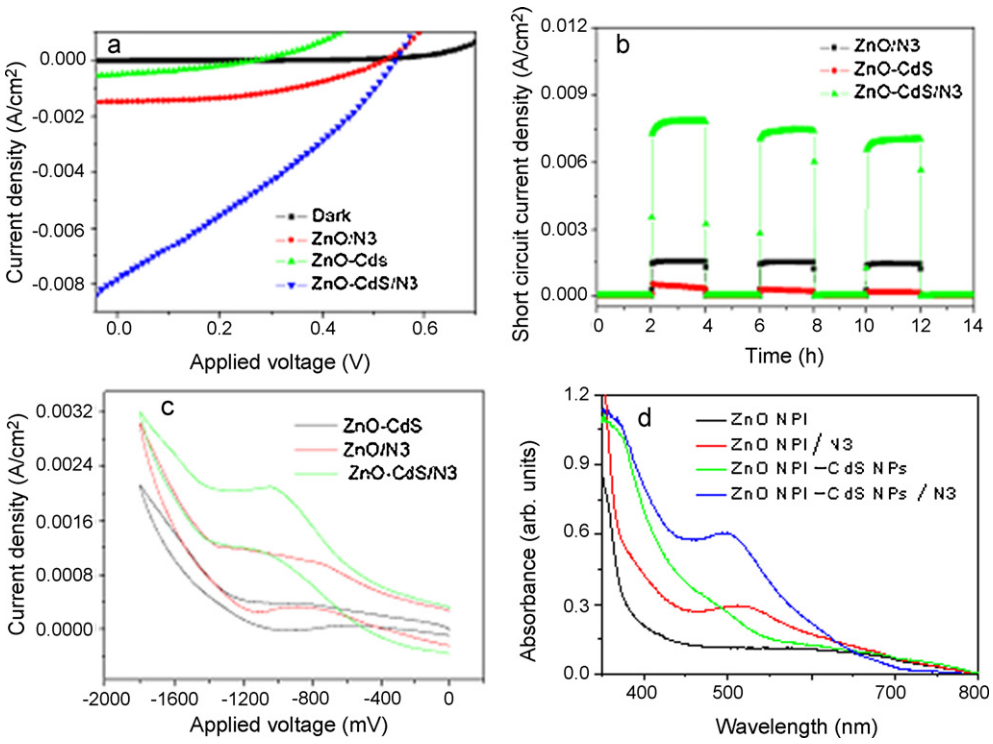

Fig. 2. (a) Plot of current density as function of applied voltage, (b) short circuit current density as a function of time, (c) cyclic-voltammetry curves, and optical absorbance of electrodes specified as insets.

missing. In ZnO NPl–CdS NPs/N3 electrode, presence of both CdS NPs and N3 peaks revealing the formation of effective cascading system with enhanced absorbance. This would have boosted overall performance of ZnO NPl–CdS NPs + N3 electrode compared with other three.

4. Conclusions

In conclusion, this work demonstrates the advantage of CdS nanoparticles and N3 dye in ZnO-based DSSCs systems. The X-ray diffraction, SEM analysis and EDX measurements are operated for confirming the phase, surface morphology and elemental stoichiometry. The attachment of the CdS nanoparticles with the ZnO nanoplates is confirmed from the low resolution TEM image whereas, straight fringes correspond to lattice spacing of ZnO structure are also evidenced from the high resolution TEM image. Enhanced photosensitization followed by optical absorbance by involving organic and inorganic photosensitisers is achieved. In the presence of CdS quantum dots between ZnO and N3 both cell performance and the stability are improved. This also alleviates the issues leading to CdS photocorrosion and Zn^{2+}/dye complex layer formation (surface aggregation). The improvement in the solar-to-electrical conversion efficiency from 0.36 and 0.04 to 1.3% supports fast electron injection kinetics through the cascade steps.

Acknowledgements

This work was supported by the Korea Foundation for International Cooperation of Science and Technology (KICOS) through a grant provided by the Korean Ministry of Science and Technology (MOST) in No. K20501000002-07-E0100-00210 and the New & Renewable Energy program of the Korea Institute of Energy Technology Evaluation and Planning (KETEP) grant (No. 20103020010050) funded by the Ministry of Knowledge Economy, Republic of Korea.

References

[1] H.J. Snaith, L. Schmidt-Mende, Adv. Mater. 19 (2007) 3187.
[2] A. Otsuka, K. Funabiki, N. Sugiyama, T. Yoshida, Chem. Lett. 35 (2006) 666.
[3] M. Law, L.E. Greene, J.C. Johnson, R. Saykally, P.D. Yang, Nat. Mater. 4 (2005) 455.
[4] J.B. Baxter, E.S. Aydil, Appl. Phys. Lett. 86 (2005) 53114.
[5] M. Gratzel, J. Photochem. Photobiol. C: Photochem. Rev. 4 (2003) 145.
[6] A.B.F. Martinson, J.W. Elam, J.T. Hupp, M.J. Pellin, Nano Lett. 7 (2007) 2183.
[7] R. Liu, A.A. Vertegel, E.W. Bohannan, T.A. Sorenson, J.A. Switzer, Chem. Mater. 13 (2001) 508.
[8] M. Shaheer Akhtar, M. Alam Khan, M. Seok Jeon, O.B. Yang, Electrochim. Acta 53 (2008) 7869.
[9] K. Leschkies, R. Divakar, J. Basu, E. Enache-Pommer, J. Boercker, C. Carter, U. Kortshagen, D. Norris, E. Aydil, Nano Lett. 7 (2007) 1793.
[10] J.C. Lee, W.J. Lee, S.H. Han, T.G. Kim, Y.M. Sung, Electrochem. Commun. 11 (2009) 23.
[11] W.J. Lee, W.C. Kwak, S.K. Min, J.C. Lee, W.S. Chae, Y.M. Sung, S.H. Han, Electrochem. Commun. 10 (2008) 1699.
[12] W.J. Lee, S.H. Kang, S.K. Min, Y.E. Sung, S.H. Han, Electrochem. Commun. 10 (2008) 1579.
[13] W.J. Lee, R.S. Mane, S.H. Lee, S.H. Han, Electrochem. Commun. 9 (2007) 1502.
[14] K.R. Gopidas, M. Bohorquez, P.V. Kamat, J. Phys. Chem. 94 (1990) 6435.
[15] J.E. Evans, K.W. Springer, J.Z. Zhang, J. Phys. Chem. 101 (1994) 6222.
[16] H. Fujii, M. Ohtaki, K. Eguchi, H. Arai, J. Mol. Catal. A: Chem. 129 (1998) 6.
[17] P.V. Kamat, Chem. Rev. 93 (1993) 267.
[18] R.S. Mane, C.D. Lokhande, Mater. Chem. Phys. 65 (2000) 1.
[19] R.S. Mane, H.M. Pathan, W.J. Lee, S.H. Han, J. Phys. Chem. B 109 (2005) 24254.
[20] W. Lee, S.K. Min, S. Shin, S.H. Han, S.H. Lee, Appl. Phys. Lett. 92 (2008) 23507.
[21] S.C. Lin, Y.L. Lee, C.H. Chang, Y.J. Shen, Y.M. Yang, Appl. Phys. Lett. 90 (2007) 14351.
[22] C.H. Chang, Y.L. Lee, Appl. Phys. Lett. 91 (2007) 053503.
[23] T. Ganesh, R.S. Mane, C. Gangri, J.H. Chang, S.H. Han, J. Phys. Chem. C 113 (2009) 7666.
[24] S.B. Ambade, R.S. Mane, A. Ghule, M.G. Takwale, A. Abhyankar, Scripta Mater. 61 (2009) 12.
[25] Y.L. Lee, C.H. Chang, J. Photochem. Photobiol. A: Chem. 185 (2008) 584.